KAUNAS UNIVERSITY OF TECHNOLOGY
VILNIUS GEDIMINAS TECHNICAL UNIVERSITY

ROLANDAS GIRČYS

DEVELOPMENT AND STUDY OF A WEARABLE REAL-TIME HEMODYNAMIC PARAMETER MONITORING SYSTEM

Summary of Doctoral Dissertation
Technological Sciences, Informatics Engineering (07T)

2016, Kaunas

Doctoral dissertation was prepared in Kaunas University of Technology, Centre of Real Time Computer Systems during the period 2009–2016.

The dissertation is defended externally.

Scientific Advisor:
Prof. Dr. Egidijus KAZANAVIČIUS (Kaunas University of Technology, Technological Sciences, Informatics Engineering – 07T).

Dissertation Defence Board of Informatics Engineering Science Field:
Prof. Dr. Rimvydas SIMUTIS (Kaunas University of Technology, Technological Sciences, Informatics Engineering – 07T) – **chairman;**
Prof. Dr. Eugenijus KANIUŠAS (Vienna University of Technology, Technological Sciences, Informatics Engineering – 09P);
Prof. Dr. Algimantas KRIŠČIUKAITIS (Lithuanian University of Health Sciences, Biomedical Sciences, biophysics – 02B);
Assoc. Prof. Olga KURASOVA (Vilnius University, Technological Sciences, Informatics Engineering – 07T);
Prof. Dr. Dalius NAVAKAUSKAS (Vilnius Gediminas Technical University, Technological Sciences, Informatics Engineering – 07T).

English Language Editor: Aušra Vrubliauskaitė-Fratila

The official defence of the dissertation will be held at 10 a.m. on October 28, 2016 at the public meeting of Dissertation defence board of Informatics Engineering science field in Dissertation Defense Hall at Kaunas University of Technology.

Address: K. Donelaičio St. 73, LT-44249 Kaunas, Lithuania.
Tel. no (+370) 37 300 042; e-mail doktorantura@ktu.lt

Summary of doctoral dissertation was sent on 28th September, 2016.
The doctoral dissertation is available on the internet http://ktu.edu, at the library of Kaunas University of Technology (K. Donelaičio St. 20, LT-44239 Kaunas, Lithuania) and at the library of Vilnius Gediminas Technical University (Saulėtekio al. 14, LT-10223 Vilnius, Lithuania).

KAUNO TECHNOLOGIJOS UNIVERSITETAS
VILNIAUS GEDIMINO TECHNIKOS UNIVERSITETAS

ROLANDAS GIRČYS

DĖVIMOS, REALAUS LAIKO KRAUJOTAKOS PARAMETRŲ STEBĖJIMO SISTEMOS SUDARYMAS IR TYRIMAS

Daktaro disertacijos santrauka
Technologijų mokslai, informatikos inžinerija (07T)

2016, Kaunas

Disertacija rengta 2009–2016 metais Kauno technologijos universiteto, Realaus laiko kompiuterių sistemų centre.

Disertacija ginama eksternu.

Mokslinis konsultantas:
Prof. dr. Egidijus KAZANAVIČIUS (Kauno technologijos universitetas, technologijos mokslai, informatikos inžinerija – 07T).

Informatikos inžinerijos mokslų krypties disertacijos gynimo taryba:
Prof. dr. Rimvydas SIMUTIS (Kauno technologijos universitetas, technologijos mokslai, informatikos inžinerija – 07T) – **pirmininkas;**
Prof. dr. Eugenijus KANIUŠAS (Vienos technologijos universitetas, technologijos mokslai, informatikos inžinerija – 09T);
Prof. dr. Algimantas KRIŠČIUKAITIS (Lietuvos sveikatos mokslų universitetas, biomedicinos mokslai, biofizika – 02B);
Doc. dr. Olga KURASOVA (Vilniaus universitetas, technologijos mokslai, informatikos inžinerija – 07T);
Prof. dr. Dalius NAVAKAUSKAS (Vilniaus Gedimino technikos universitetas, technologijos mokslai, informatikos inžinerija – 07T).

Anglų kalbos redaktorė: Aušra Vrubliauskaitė-Fratila

Disertacija bus ginama viešame Informatikos inžinerijos mokslo krypties disertacijos gynimo tarybos posėdyje 2016 spalio 28d. 10val. Kauno technologijos universiteto, Disertacijų gynimo salėje.

Adresas: K. Donelaičio g. 73, LT-44249 Kaunas, Lietuva.
Tel. (8 37) 300042; el. paštas doktorantura@ktu.lt

Disertacijos santrauka išsiųsta 2016m. rugsėjo 28 d.
Su disertacija galima susipažinti internetinėje svetainėje http://ktu.edu, Kauno technologijos universiteto bibliotekoje (K. Donelaičio g. 20, LT-44239 Kaunas) ir Vilniaus technikos universiteto bibliotekoje (Saulėtekio al. 14, 10223 Vilnius).

1. INTRODUCTION

Cardiovascular diseases are the leading cause of mortality in the world. According to data provided by the World Health Organization, mortality from cardiovascular diseases in 2005 – 2015 accounted for 56% of all global deaths. On the other hand, life expectancy is increasing in the world, which leads to the increasing numbers of older individuals as compared to other age groups. In order to avoid the rise of healthcare costs, more and more individuals are treated at homes and more attention is given to disease prevention. These tendencies show that it is important to create new devices and methods for continuous monitoring of hemodynamic parameters throughout the day, and to look for new reliable indicators that would improve the prognosis of circulatory disorders.

Justification of the research problem. Non-invasive hemodynamic test methods, such as magnetic resonance imaging, ultrasound, impedance cardiography, are used only in clinical practice. That is because the devices used to implement these methods are expensive, complex and largely meant for purposes of diagnosis. The majority of commercial devices for outpatient use implement the auscultatory method and tonometry. These are non-invasive / occlusive methods, but they have the following shortcomings:

1) Method implementation requires external pressure to be put on the blood vessel segment. Usually, an inflatable sleeve is used for that purpose. Therefore, only momentary values are recorded and the recording period does not exceed a few dozen seconds;

2) This method is unsuitable for long-term monitoring because continuous external pressure would damage soft tissues and create discomfort for the patient.

Currently known non-occlusive hemodynamic parameter measurement methods are classified into: 1) methods that register two processes (usually, an electrocardiogram and arterial pulse wave), 2) methods that register one process – the arterial pulse wave.

The main drawback of the first group of methods – the need to register two signals. Converting analog signals of two output sensors into digital signals requires two ADCs or additional devices for the realization of a two-channel ADC. In addition to that, supplementary computing resources are required for real-time digital signal processing of two signals. Using two sensors leads to additional issues: restricted placement of sensors on the surface of the body and difficulty of embedding the sensors into a device worn during daily activities (a watch, a bracelet, etc.).

The main drawback of the second group of methods – the amount of computing resources needed for their implementation is too large to apply in wearable devices. This and other aspects encourage the quest for new solutions.

1.1. Research Object

The object of this dissertation is non-invasive methods for measurement and processing of hemodynamic parameters.

These systems are based on digital processing of physiological signals. Signal parameters obtained during processing are then used in mathematical models that help calculate hemodynamic parameters.

Change in arterial volume, diameter or arterial pressure (a physiological signal) during a cardiac cycle (the time between two heartbeats) is known as the arterial pulse wave (APW). This wave is produced from the interaction between the heart and the arterial system. Therefore, the parameters of this wave (both in terms of time and rate) reflect the condition of the arterial system, whereas the interdependence between APW parameters and hemodynamic processes are described by physical-mathematical models. In order to find APW parameters, digital signal processing is performed.

The main issue that arises when developing wearable systems for continuous 24/7 monitoring of hemodynamic parameters – *limited computing and energy resources*. Such systems (a watch, a bracelet, etc.), apart from serving a functional purpose, also have an aesthetic function, therefore, the size of these systems limits the energy and calculation resources meant for its functional purpose.

Today, efficient processors for signal processing are available on the market, as well as analog-to-digital converters with high resolution and sampling frequency. Analog-to-digital conversion and digital signal processing consumes the major part of computing and energy resources of the system. This significantly reduces the time for continuous monitoring of hemodynamic parameters. Therefore, new solutions are needed in order to develop wearable systems that can be worn during daily activities, and can monitor the condition of the arterial system on a continuous basis, 24/7. Finding these solutions include: 1) search for values of APW parameters that require less computational resources than the ones in use today, 2) development of mathematical-physical models that link the APW and hemodynamic parameters, 3) development of noise-resistant subsystems for analog signal input that do not use ADC (analog-digital converter), 4) development of noise-resistant methods for assessment of APW parameter values.

The solutions to the aforementioned tasks are closely related to the development of wearable systems for hemodynamic parameter monitoring, but can be used in other areas as well.

1.2. Research Goal and Tasks

Research goal – development and testing of arterial pulse wave analysis methods used for calculating hemodynamic parameters, and development and testing of a real-time system used for continuous (24/7) hemodynamic parameter monitoring with a noise-resistant signal input subsystem.

Research Tasks:

1. Review and analyze non-invasive methods for measurement and processing of hemodynamic parameters.
2. Create mathematical models that link hemodynamic and APW front edge parameters.
3. Develop noise-resistant solutions for calculating the APW front edge parameter values.
4. Develop a structure and an algorithm for the noise-resistant, energy-saving signal input subsystem.
5. Create a structural model of a wearable real-time system for measurement and processing of hemodynamic parameters.

1.3 Research Methodology

Experimental verification of hemodynamic parameter measurement methods is performed with a veloergometry test (physical tolerance test), during which photoplethysmography, electrocardiogram and blood pressure is measured.

1.4. Scientific Novelty

1. Mathematical models that link the steepness of the APW front edge with its propagation speed and arterial blood pressure were created.
2. A new method for determining the starting point of the APW is proposed. Application of this method produces results that are more accurate, and have a lower level of scatter as compared to other known methods.
3. A novel structure of a noise-resistant photoplethysmographic signal input subsystem is proposed.

1.5. Thesis Statements

1. Steepness of the deformation pulse wave front edge correlates with its propagation speed and blood pressure.
2. Energy consumption is reduced when analyzing only the front edge of APW in order to find hemodynamic parameter values.
3. A light flux modulated with an optical Barker code, which is used in a photoplethysmographic sensor, allows a significant decrease of noise in the output signal of the sensor. It also allows avoiding continuous

filtering of a digital signal, which, in turn, reduces energy consumption of the wearable system.

4. When analog-to-digital converter is replaced with a “light flux – time” converter, energy consumption of the wearable system is reduced.
5. When applying linear approximation of the APW foot, impact of noise on the estimation of the APW starting point is significantly reduced.

1.6. Practical Significance

Modern semiconductor light sources and sensors, which are safe, small and low cost, can be used to implement the photoplethysmographic peripheral hemodynamic parameter registration method. This method is best suited to meet the requirements posed to devices meant for outpatient and home use.

Methods for APW front edge analysis developed in this paper, as well as application of a modulated light flux photoplethysmographic sensor provides wider opportunities for a more rational use of critical resources in wearable systems (such as energy consumption and computational resources).

1.7. Research Approbation

Research results were applied in software developed for a smart home environment under the project "Research on Smart Home Environment and Development of Intelligent Technologies (BIATech)", VP1−3.1−ŠMM−10−V−02−020.

Research results were applied in a project sponsored by Agency for Science, Innovation and Technology (MITA), project Nr. VP2-1.3-ŪM-05-K-01-147, 2013 “Research and development of human-machine interfaces using computational intelligence techniques”.

Works published under the topic of the dissertation:

1. Girčys, R., Liutkevičius, A., Vrubliauskas, A., & Kazanavičius, E. (2015) Blood pressure estimation according to photoplethysmographic signal steepness. Information technology and control, 44(4), p. 443-450.
2. Girčys, R., Kazanavičius, E., Vrubliauskas, A., & Liutkevičius, A. (2014). Movement artefact resistant photoplethysmographic probe. Electronics and Electrical Engineering, 20(3), 73-76.
3. Girčys, R., Kazanavičius, E., Obcarskas, L. (2013) Arterial pulse transit time evaluation by peripheral pulse wave measurement. Journal of measurements in engineering, 1(1), p. 52-58.
4. Kazanavičius, E., Girčys, R., Vrubliauskas, A., & Lugin, S. (2005) Mathematical methods for determining the foot point of the arterial pulse wave and evaluation of proposed methods. Information technology and control, 34(1), p. 29-36.

5. Girčys, R., Kazanavičius, E., Lugin, S., & Vrubliauskas, A. Mathematical model of the aortic root pressure waveform as an input function of the arterial system. Mechanika, 2(46), p. 42-45.

1.7. Dissertation Structure

The dissertation consists of an introduction, four chapters, dissertation conclusions, references and annexes. The dissertation text is 116 pages long.

Content. Justification of the research object, relevance, goal, tasks, novelty and significance of the work are given in the Introduction, along with an outline of defended thesis statements.

A review and analysis of non-invasive methods for blood pressure and deformation pulse wave registration, as well as hemodynamic parameter calculation methods are given in Chapter 2.

Mathematical-physical models created by the author that link the APW front edge with blood pressure parameters can be found in Chapter 3, Subchapter 1.

In Chapter 3, Subchapter 2, methods for determining the starting point of a photoplethysmographic signal (PPG) are realized in a digital data processing subsystem. Analysis is performed on the impact that noise has on the accuracy and cohesion of received results.

The photoplethysmographic signal input subsystem, which significantly reduces noise level in PPG sensor output, is described in Chapter 3, Subchapter 3. Algorithm “light flux – time”, which allows the digitalization of the signal without the standard ADC, is described.

A description of the wearable hemodynamic parameter monitoring system (WHPMS) structure with a noise-resistant PPG analog input subsystem is given in Chapter 3, Subchapter 4. Energy consumption levels of the input subsystem are analyzed. The impact the created mathematical models have on the energy consumption of WHPMS is studied.

A description of a WHPMS prototype with blood pressure and PWV (pulse wave velocity) calculation methods created by the author and implemented in the WHPMS is given in Chapter 4, Subchapter 1.

Experiment for the verification of mathematical models for blood pressure and PWV calculation methods created by the author is described in Chapter 4, Subchapter 2. Experiment results and conclusions regarding the concordance of results received with proposed and with known methods are also given in this chapter.

2. NON-INVASIVE METHODS FOR MEASUREMENT OF HEMODYNAMIC PARAMETERS

The circulatory system consists of two main elements: the heart and the arterial system. A pressure pulse wave (PPW) and a deformation pulse wave (DPW) are produced as a result of their interaction Figure 2.1 (a). Registration and analysis of these waves allows defining such circulatory parameters as blood pressure and values of arterial stiffness.

The arterial system performs the functions of an “elastic reservoir” and blood “transportation”. Because of the “elastic reservoir” function, the potential energy generated during the systole phase is absorbed by the arterial walls, and is then used for blood transportation via the arterial system in the diastolic phase.

Whether this function is performed effectively depends on the ability of the artery to deform, i.e. arterial stiffness. Stiffness values can be calculated if the strain-stress characteristics are known. However, the latter cannot be measured within a live organism *in situ*.

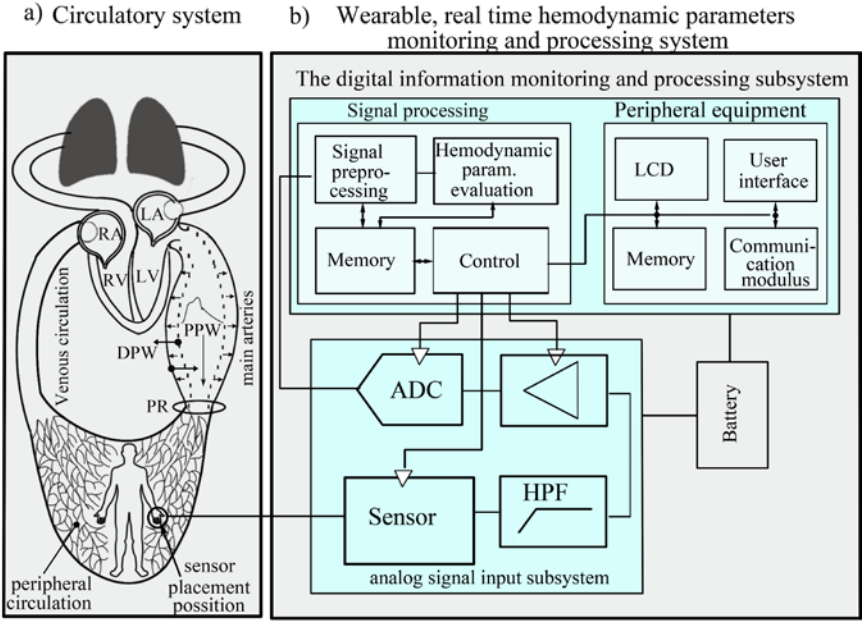

Figure 2.1 Arterial circulation and the structure of a wearable real-time hemodynamic parameter monitoring and processing system; a) arterial circulation system: left atrium (LA), right atrium (RA), left ventrical (LV), right ventrical (RV), pressure pulse wave (PPW), deformation pulse wave (DPW), peripheral resistance (PR); b) hemodynamic parameter monitoring and processing system

Assuming that the PPW is strain force and the DPW – deformation, to measure stiffness in Figure 2.1(a), the following quantitative stiffness input values are calculated: compliance, distensibility, Peterson modulus, DPW pulse wave velocity (PWV) or pulse transit time (PTT). These input values characterize the ability of an artery (as an elastic reservoir) to deform. In order to find these values, registration of PPW and DPW is necessary.

2.1. Non-Invasive Deformation and Pressure Pulse Waves Registration Methods

Most commonly used methods for registration of changes in the arterial geometry (DPW) during a cardiac cycle are given in Table 2.1. Some of these methods are used to measure momentary min / max values during a cardiac cycle. Other methods are used to register all DPW values that fall under a cardiac cycle.

The DPW is registered with ultrasound and photoplethysmography. With ultrasound, both the trajectory of the DPW and the values of its amplitude in millimeters are obtained. Even though this is a significant advantage, application of this method is not suitable in WHPMS. When a DPW is registered with photoplethysmography, a trajectory of the DPW is produced, and it can be registered continuously – 24/7. Modern semiconductor technology enables the photoplethysmographic method to be integrated in electronic jewelry and thus be used in WHPMS.

Table 2.1 Comparison of non-invasive DPW registration methods

Method	Used in	VpC	Long-term	Experience	Measures
Ultrasound	Health institutions	DPW	No	Yes	Diameter dim(m)
Magnetic resonance imaging	Health institutions	min/max	No	Yes	Diameter dim(m)
Computed tomography scan	Health institutions	min/max	No	Yes	Diameter dim(m)
Photoplethysmography	Outpatient	DPW	Yes	No	Trajectory of volume change dim(mV)

NRP – number of registered processes, VpC – number of values per cardiac cycle, min – lowest DPW value during a cardiac cycle, max – highest DPW value during a cardiac cycle, DPW – deformation pulse wave.

Arterial occlusion is necessary when applying non-invasive PPW registration methods Table 2.2.

The PPW form (all blood pressure parameters per cardiac cycle) can only be measured with tonometry and volume compensation methods (*Penaz*). However, because these methods require pressure to be applied on the surface of the skin (occlusion), they are not suitable for *real-time* (registration of each

Table 2.2 Comparison of arterial blood pressure registration methods

Method	Arterial occlusion	RpK	Number of sensors	Experience
Auscultatory (Korotkoff)	Full, periodic	SBP, DBP	2	Necessary
Oscillometric	Full, periodic	SBP, DBP	1	Not necessary
Tonometry	Partial, continuous	PPW	1	Not necessary
Volume compensation (Penaz)	Partial, continuous	PPW	1	Not necessary

RpK – number of values per cardiac cycle, PPW – pressure pulse wave values.

heartbeat) hemodynamic parameter monitoring systems that are worn during daily activities. When other methods are used, the PPW form and all the information it carries is no longer available.

The analysis of non-invasive DPW and PPW registration methods shows that photoplethysmographic DPW registration is best suited for use in WHPMS, and digital PPG analysis – for hemodynamic parameter calculation.

2.2. Analysis of the Photoplethysmographic Signal for the Measurement of Hemodynamic Parameters

When the DPW is registered with a photoplethysmograph in the periphery of the arterial system, a photoplethysmographic signal (PPG) is produced.

When analyzing a PPG, the following arterial stiffness indexes are found: pressure augmentation index, reflection index, stiffness index. When the Windkessel model is used for analysis, stiffness parameters of the main and peripheral arteries are calculated. The stiffness of the arterial system is also reflected by the DPW propagation speed, which is calculated by registering two DPWs at different points.

PPG analysis also produces arterial blood pressure values. For this purpose, a neural network is used: its input parameters are the values of time

moments when characteristic PPG points appear during a cardiac cycle. There are methods for measuring arterial blood pressure by analyzing time moment values of when characteristic second derivative PPG points appear during a cardiac cycle.

When PPG is analyzed to calculate blood pressure values, the entire PPG that falls into a cardiac cycle is analyzed. The analysis of all PPG values per cardiac cycle is not rational because it consumes precious computing and energy recourses. Therefore, there is a clear need for methods that would allow calculation of arterial blood pressure and stiffness values by analyzing only a part of the PPG.

2.4. Energy Consumption of a Wearable Real-Time System for Hemodynamic Parameter Monitoring

In systems that implement the photoplethysmographic DPW registration method, the entire PPG that falls into a cardiac cycle is analyzed.

Hemodynamic parameter values are found in the following three stages:

1) preparation of the photoplethysmographic signal,
2) obtainment of PPG parameter values,
3) calculation of hemodynamic parameters.

In the signal preparation stage, the following adaptive filtering methods are used: adaptive mean square method, recursive mean square method, Wiener f. Kalman f., Independent component analysis method. If a row of mentioned filters is L = 64, then the number of operations N_{op} needed to update the coefficients is $3072 \leq N_{op} \leq 275540$. If the discretization period of the PPG is T_d = 1ms, and energy consumption for the current is I_{proc} = 137μA/MHz *(*ARM STM32 Cortex M4*)*, then the energy consumed when updating filter coefficients is $1.69\text{mA} \leq I_{proc} \leq 37.75\text{mA}$. Energy consumed by the processor with an integrated ADC for analog-to-digital signal conversion is I_{ADC} = 1.8mA.

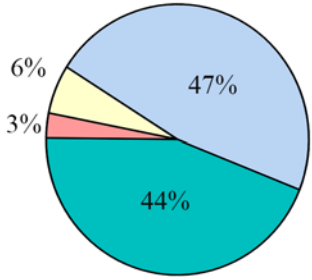

Figure 2.2 Energy consumed by the subsystems of a wearable hemodynamic parameter monitoring system: 1) analog-to-digital converter 47%, 2) processor (digital filtering and analysis) 44%, 3) photoplethysmographic sensor 6%, 4) remaining WHPMS subsystems (user interface, communication module (active 4s/24h), DC-DC converter, analog signal processing) 3%

Assuming that L=32 row least mean square FIR (finite impulse response) filter is used for signal preparation, then the energy consumption distribution of the WHPMS is as given in Figure 2.2.

If two "tablet" type 3.3V batteries are used to power the system (for example, CR2032 with the capacity of 250mAh), then the operation time of the WHPMS is (2×250)mAh/3.83mAh = 130 hours (~5 days). If a 3.3V lithium battery with 1250mAh capacity is used (Lithium, Ultra High Capacity), the WHPMS will function (2×250)mAh/3.83mAh = hours (~14 days).

The analysis shows, as seen in Figure 2.2, that the major part of energy consumed by the wearable hemodynamic parameter monitoring system is allocated to the following three functions: 1) analog-to-digital conversion, 2) digital signal filtering, 3) photoplethysmographic sensor.

Analog-to-digital conversion and adaptive filtering need to be performed continuously, as a result – taking up 80% of all energy resources. Therefore, *new solutions are needed to reduce energy consumption of these two subsystems*.

2.5. Conclusions

1. The forms of PPW and DPW, created from the interaction between the heart and the arterial system, provides information about the condition of the circulatory system. Analysis of these waves provides information not only about the blood pressure in the arterial network, but the arterial stiffness input parameters as well.
2. Methods used to measure separate blood pressure values or to monitor the PPW are: oscillometry, tonometry and volume compensation (*Penaz*).
3. Photoplethysmography method allows registration of the DPW during the entire cardiac cycle. Unlike the PPW registration methods, this method does not have restrictions that would impede its application in wearable hemodynamic parameter registration systems in real-time while physically active.
4. The study of DPW analysis methods used to calculate hemodynamic parameters showed: 1) in order to evaluate blood pressure and stiffness of the arterial system, all DPW values that fall into a full cardiac cycle need to be analyzed, which leads to continuous preparation of the PPG signal (filtering), 2) in order to calculate the DPW propagation time/speed, two signals need to be analyzed: electrocardiogram and PPG, or PPG measured in two remote points.
5. Adaptive methods for photoplethysmographic signal preparation require significant computational resources. Performance of this task takes up to 44% of all energy needed to run the system, therefore: 1) new DPW parameters and mathematical models are needed to calculate blood

pressure and arterial stiffness values by analyzing only one part of the entire DPW, 2) noise-resistant PPG input system.

6. Conversion of analog PPG to a digital one with ADC integrated in the processor consumes up to 47% of all energy resources, therefore: 1) new solutions for analog-to-digital PPG conversion is needed, 2) new mathematical models that would allow calculating the DPW propagation time/speed by analyzing *only one signal*.

3. MATHEMATICAL MODELS REALIZED IN THE WEARABLE HEMODYNAMIC PARAMETER MONITORING SYSTEM AND ITS STRUCTURE

In this chapter, the following items are presented: 1) mathematical models that link the front edge of the PPG with hemodynamic parameters, 2) noise-resistant PPG processing method for foot point detection, 3) methodology used to create a functional algorithm of the noise-resistant analog signal input subsystem, 4) structure of a wearable hemodynamic parameter monitoring system (WHPMS), in which the analog signal input subsystem does not need an ADC and the digital information processing subsystem does not perform signal preprocessing.

3.1. Mathematical Models that Link Hemodynamic and the Deformation Pulse Wave Front Edge Parameters

Selection of a signal analysis method and the complexity of the functional algorithm depend on PPG parameters used in the mathematical model. Therefore, when developing WHPMS, it is important to choose mathematical models with parameters that require less algorithm complexity and lower computational resources.

3.1.1. Mathematical Model that Links the Arterial Blood Pressure and the Duration of the Pulse Wave Front Edge

A mathematical model that links the duration of the front edge of a PPG with arterial pressure is presented in this chapter.

Arterial pulse waves are created from the interaction of the action F_A and the reaction F_R forces that are generated by the arterial system and the left ventricle. According to the force balance equation:

$$\sum F_A + \sum F_R = 0\,, \tag{3.1}$$

the following mathematical model was developed:

$$P = \frac{\rho \cdot \eta \cdot dv \cdot ds \cdot \left(m_a l + M \cdot x\right)}{\Delta t \cdot m \cdot dF}\,; \tag{3.2}$$

here m –blood mass, η –dynamic viscosity, dF –fraction in blood flow, ρ –blood density, dv –blood flow velocity deviation, ds –arterial cross-section deviation, Δt – APW front edge duration, M –left ventricle mass, x –cardiac wall motion amplitude, m_a –arterial wall mass.

According to (3.2), the highest the blood pressure during the cardiac cycle is inverse proportional to APW front edge duration.

3.1.2. Mathematical Model that Links the Arterial Blood Pressure and the Steepness of the Deformation Pulse Wave Front Edge

The mathematical model for coupling the arterial blood pressure and the DPW front edge steepness.

This section describes a mathematical model linking the DPW front edge steepness and blood pressure.

The systolic blood pressure (p_i) at i-th cardiac cycle can be found using formula:

$$p_i = K \cdot \mathrm{tg}(\gamma_i); \tag{3.3}$$

here $tg(\gamma_i)$ – DPW front edge steepness, dim(γ_i) =degree, K – constant, dim(K) = $L^{-1}MT^2$.

Coefficient K_i value is:

$$K_i = 1334 \cdot \frac{h \cdot \left(p_{sys} - p_{dias}\right)}{\left(d_{\max} - d_0\right)} \cdot \ln\left(t_i\right). \tag{3.4}$$

here t_i – DPW duration of the front edge during i-th cardiac cycle, h – arterial wall thickness, p_{sys} – systolic blood pressure, p_{dias} – diastolic blood pressure. The coefficient K and blood pressure has same dimensions dim(K)=dim(P) =$L^{-1}MT^{-2}$.

3.1.3. Mathematical Model that Links the Propagation Speed of the Deformation Pulse Wave and the Steepness of Its Front Edge

According to the force balance equation balance law the mathematical model of the arterial wall movement velocity was developed:

$$v_r = tg(\varphi) = dl/dt = \sqrt{(E/m)\sqrt{\left(l^2 - \Delta l^2\right)}}; \tag{3.5}$$

here φ – the DPW front edge steepness, dl – the arc length of the arterial cross-section, E – Young modulus, m – the mass of the arterial wall, l – the initial arc length of the arterial cross-section;

The model shows, that radial arterial wall movement velocity v_r, as the DPW propagation through arterial system velocity v_x (Moens-Korteveg eq.):

$$v_x = \sqrt{Eh/\rho l}\ , \tag{3.6}$$

depend on the Young modulus E and variates in same manner. Therefore, the v_r, can be used as v_x when monitoring the dynamics of the arterial wall stiffness.

3.1.4. Verification of Mathematical Models for Hemodynamic Parameter Calculation

Verification of the developed mathematical models was carried out in MatLab environment using the Windkessel model:

$$p(t) = h(t) * Q(t), \tag{3.7}$$

$$h(t) = a_1 e^{-a_2 t} + a_3 e^{-a_4 t} \cos(a_5 t - a_6), \tag{3.8}$$

here – $Q(t)$ blood debit at systole, $h(t)$ –arterial system transfer function, and "pressure – deformation" function:

$$d(t) = d_0 \ln(p(t) - \ln(p_0) + 1), \tag{3.9}$$

generated the pressure $p(t)$ and the deformation $d(t)$ pulse waves. Time axis step duration – 1ms.

In an arterial system that does not have the "elastic reservoir" function, blood pressure values were calculated in the following way:

$$P_1(t) = Q(t) \cdot R\ , \tag{3.10}$$

here – R peripheral resistance.

3.1.4.1. Verification of the Mathematical Model that Links the Arterial Blood Pressure and the Duration of the Pulse Wave Front Edge

The model was verified by comparing pulse pressure values calculated according to the Windkessel (3.7) and the model created by the author (3.2).

Because values $P_2(i)$ and $P_1(i)$ produced during modeling are different Figure 3.1 (a), their trajectories were compared by mapping $P_2(i)$ and $P_1(i)$ to interval $[0,1]$.

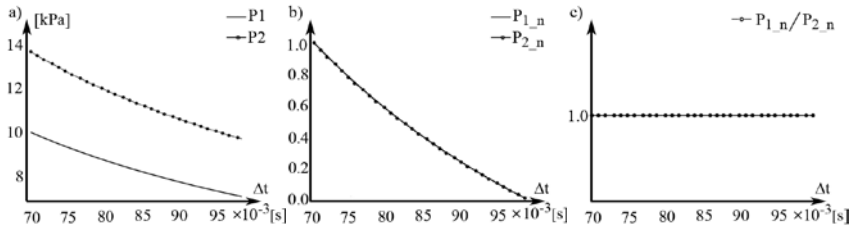

Figure 3.1 a) pressure values P_2 were calculated using the original model *(3.2)*, and values P_1 – using (3.7), b) trajectories of values P_{1_n} and P_{2_n} are identical, c) values P_1 and P_2 differ by a constant A

Identical trajectories Figure 3.1(b) and ratio $P_{1\_n}/P_{2\_n} = 1$ show that highest blood pressure values registered using the model created by the author (3.2) and the standard model (3.10) differ by a constant.

Model developed by the author (3.2) can be used to monitor blood pressure *dynamics*, but because of the front edge duration and non-linear blood pressure dependence it is not suitable to measure blood pressure values.

3.1.4.2. Verification of the Mathematical Model that Links the Arterial Blood Pressure and the Steepness of the Deformation Pulse Wave Front Edge

The pressure pulse waves $P_{3i}(t)$ were generated according to (3.7), and their highest amplitude values were varied by sine law in interval ($14.5\text{kPa} \leq P_{3i}(t) \leq 24\text{kPa}$). The corresponding deformation pulse waves were generated according to (3.9). Using the original model (3.3, 3.4), pressure values $P_4(i)$ and $P_3(i)$ were calculated and are shown in Figure 3.2(a). The correlation coefficient r=0.998 (Pearson method) shows significant correspondence between the $P_4(i)$ and $P_3(i)$ trajectories. Root mean square error was 0.254kPa with confidence interval [0.242kPa, 0.266kPa] when confidence level was 95%.

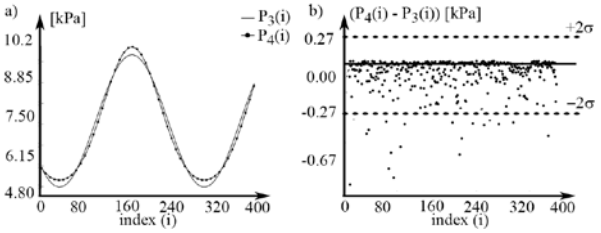

Figure 3.2 Comparison of pressure values $P_3(i)$ calculated using the Windkessel model and pressure values $P_3(i)$ calculated using the original model: a) trajectories of $P_3(i)$ and $P_4(i)$ coincide; b) comparison of pressure values $P_3(i)$ and $P_4(i)$ using the Bland–Altman method

Blood pressure values $P_4(i)$, and $P_3(i)$ were compared using the Bland–Altman method. The mean difference between $P_4(i)$, and $P_3(i)$ was 0.133kPa, double standard deviation – ±0.27kPa Figure 3.2.(b).

The obtained results satisfy the AAMI and BHS requirements posed on outpatient blood pressure monitors. Therefore, the developed method (3.3, 3.4) can be used to measure blood pressure values in each cardiac cycle.

3.1.4.3. Verification of the Mathematical Model that Links the Steepness of the Pulse Wave Velocity and the Deformation Pulse Wave Front Edge

During modeling, deformation pulse waves were generated by changing blood pressure values randomly at interval $14Pa \le P_3(i) \le 24$kPa. The v_x and v_r values were calculated according to (3.5, 3.6) equations. Results were compared using the Bland-Altman method. The modeling results Figure 3.3 indicate, that the meant of its velocities difference is insignificant (10.45 m/s). This fact means, that longitudinal and radial velocities is different.

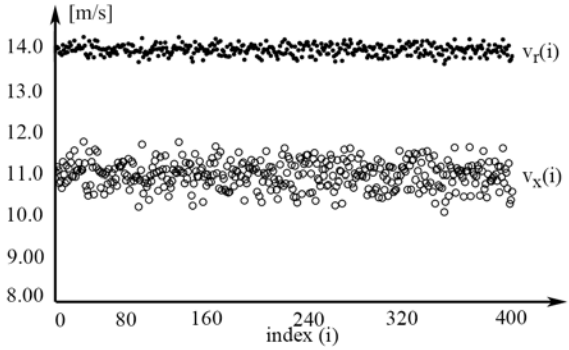

Figure 3.3 The longitudinal DPW velocity v_x and the radial arterial wall motion velocity v_r (m/s×10^{-2}) calculated using random blood pressure values

But they depend on the artery Young modulus E (3.5), (3.6) and correlate (r = 0.99). Therefore, the velocity v_r as the longitudinal velocity v_x can be used as arterial stiffness estimation.

The developed mathematical model (3.5) is acceptable for long term arterial system stiffness monitoring.

3.2. Methods for Determining the Starting Point of the Photoplethysmografic signal

This chapter presented two original methods for PPG foot point determination: One of this method named PPG foot approximation method and other – bottom straight line and forefront tangent intersection method.

PPG foot approximation method. According with this method, the first of all the search interval is determined. This interval started at ECG

(electrocardiogram) R point and finished at PPG first derivate maximum point. This interval is divided in to ten line segment. Through this segments lines are drawn using the mean square approximation method Figure 3.4. In latter stage of analysis, only the end points of those lines are used. The value of the current line starting point is added to the value of the second line starting point. In this way, the mean abscise value is calculated. The mean abscise values are approximated with a third range polynomial, and the derived curve is the PPG foot. The point at which the value of the PPG foot is lowest, is the PPG foot starting point.

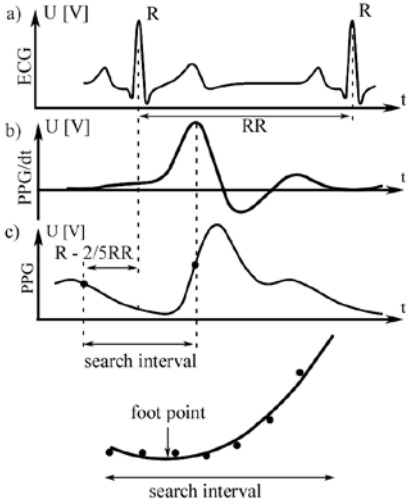

Figure 3.4 a) electrocardiogram; b) the first derivative of the DPW; c) deformation pulse wave; d) magnified view of the search interval

Bottom straight line and forefront tangent intersection method. With this method, the PPG starting point is defined as the intersection point between the bottom straight line and the forefront line tangent. Figure 3.5.

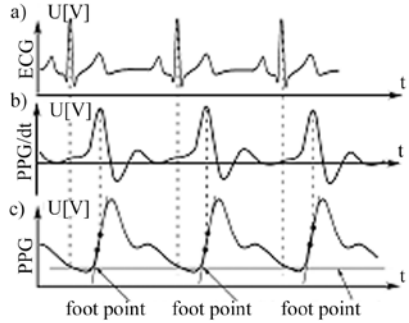

Figure 3.5 a) electrocardiogram; b) the first derivative of the PPG; c) the PPG wave

Once the PPG points that coincide with R point of the ECG are selected, the bottom straight line is drawn using the mean square method. This line is called the bottom straight line. The PPG forefront line is drawn using the PPG point at the first PPG derivative maximum and next five points back to first point. The intersection point of the bottom straight line and the forefront tangent is the starting point of the current PPG.

3.2.1. Assessing Noise-Resistance of Methods for Determining the Starting Point of the Arterial Pulse Wave

Evaluation of noise-resistance of the PPG foot point detection methods is carried out in this chapter. The less repeatability coefficient PK_k varies, the more noise-resistant the method is:

$$PK_k = \frac{1}{M} \sum_{m=0}^{M-1} pk_{mk} \,. \tag{3.10}$$

here, PK_k – repeatability coefficient for each m pairs with k conditions, M – number of pairs.

Maximum dispersion values are found using the PPG second derivative method. When there is increase of noise in the signal, the error dispersion interval varies from ±0ms to ±14ms, and the difference between the original DPW foot point and its estimation does not exceed 1ms.

When the base line-tangent intersection method is used, error dispersal values vary from ±0ms to ±11ms when noise level in the signal changes, and the difference between the *reference* value of the PPG starting point ant its input does not exceed ±6ms.

When the PPG foot approximation method is used, error dispersal values vary from ±0ms to ±6ms when noise level in the signal changes, and the difference between the *reference* value of the PPG starting point ant its input does not exceed ±1ms.

When there is noise in the signal, lowest error dispersion is achieved with the PPG foot approximation method.

3.3. Development and Testing of a Noise-Resistant Photoplethysmografic Signal Input Subsystem

In order to minimize the impact of noise on the signal, the author of this paper proposes to use a photoplethysmographic signal input subsystem. In this subsystem, the light source of the sensor emits an optical Barker code $B_0(15,5)$ = 110000000100101 generated with a method described in (Moharir & Selvarajan, 1974).

Functional algorithm of the photoplethysmographic signal input subsystem. The sequence of impulses generated by a light source is formed in

three stages. In the first stage, as shown in Figure 3.6, discretization period T_d and discretization impulse width T_L are chosen. In the second stage, every discretization impulse is divided into K sequence of impulses with a growing amplitude Figure 3.7. Value K also describes the number of quantization levels of the signal, because the range of energy intensity $E_{min} \leq E \leq E_{max}$ emitted towards the receiver is divided into K parts $\Delta = (E_{max} - E_{min})/K$, whereas the amplitude of the i-th impulse is $E[i] = i \cdot \Delta$, where $1 \leq i \leq K$. It is analogous to a b bit analog-to-digital converter, where $K = 2^b$.

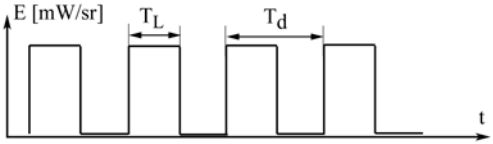

Figure 3.6 Code sequences with the length T_L are emitted in period T_d. E – intensity of the light source, T_L – impulse width, T_d – impulse period

Because the impulse period T_{imp} in the segment T_L is stable, the DPW amplitude can be expressed as a delay between the beginning of T_L and the first impulse that shows up in the receiver. This is how the converter *amplitude–time* is made.

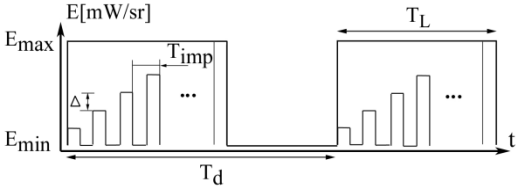

Figure 3.7 Impulses with E[i] amplitude emitted in T_{imp} period

In order to ensure that the signal received in the PPG output is noise-resistant, every impulse T_{imp} is coded in an optical code sequence B_0. To detect the coded sequence in the output of the light source, correlation between B_0 and the light receiver output is calculated. The number of correlation function spikes in the output of the correlation device corresponds with the DPW amplitude.

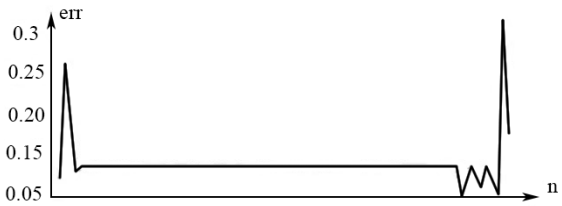

Figure 3.8 Error err values when *SNR* = 0dB

To evaluate the efficiency of the proposed method, the error was calculated Figure 3.8:

$$err = PPG - \overline{PPG}\,; \tag{3.11}$$

here PPG – photoplethysmographic signal in the output of a standard input subsystem, $\overline{\text{PPG}}$ – photoplethysmographic signal in the output of the proposed input subsystem.

Standard deviation std(err) and noise level in decibels $\text{SNR} = 20\log_{10}\left(\text{A}_{\text{sig}}/\text{A}_{\text{triuksmas}}\right)$ was measured. The efficiency of the proposed PPG probe under noisy conditions was assessed by calculating correlation values Figure 3.9.

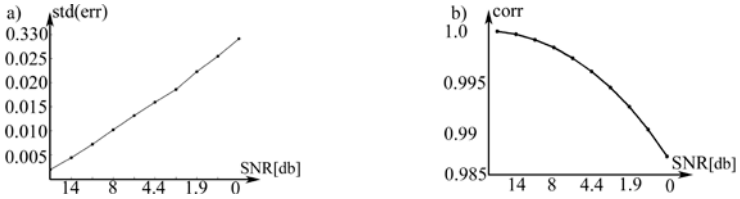

Figure 3.9 To evaluate the efficiency of the proposed method, the standard error *std(err)* of error values *err* were calculated with different noise levels (a). For the same reason, correlation values *corr* between *PPG* and $\overline{PPG}$ were calculated as well (b)

Output signal values of the standard PPG sensor and the proposed PPG sensor when SNR= 0dB are shown in Figure 3.10.

Figure 3.10 Output signal values of the standard PPG (a) and the proposed PPG (b) when SNR= 0dB

Results show that, even when the signal and noise levels are the same, when measuring the signal with the proposed method, the photoplethysmogram produced in the output retains its characteristic shape.

3.4. Wearable Hemodynamic Parameter Monitoring System with a Noise-Resistant Analog Input Subsystem

Instead of developing a software system, a special WHPMS structure was created in order to reduce energy consumption in WHPMS.

The wearable real-time hemodynamic parameter monitoring and processing system is made from the following components Figure 3.11: ARM CORTEX M4 processor, peripheral devices and a PPG signal input subsystem (PSIS) with a highly economical (power 200μW) photoplethysmographic sensor.

Communication with external devices and the PSIS is carried out via data, address and control buses. The functional algorithm of the system:

1. SYSTEM INITIALIZATION stage_1
2. ESTABLISHMENT OF PRIMARY SYSTEM PARAMETERS
3. SYSTEM INITIALIZATION stage_2
4. CALCULATION OF HEMODYNAMIC PARAMETERS
5. EXTERNAL COMMUNICATION
6. GO TO 4

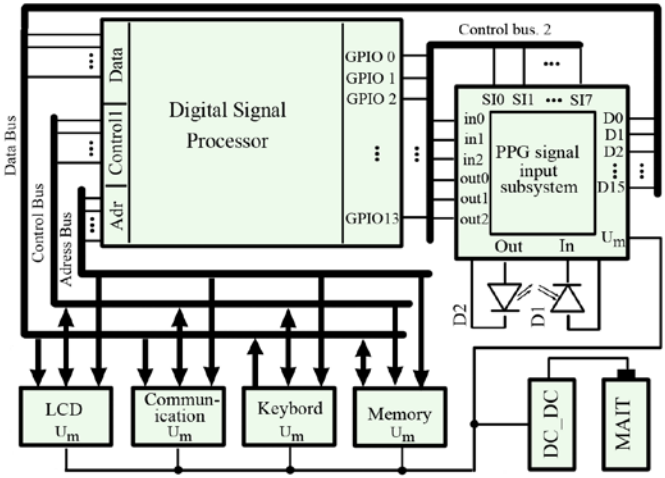

Figure 3.11 The structure of a wearable hemodynamic parameter monitoring and processing system with a noise-resistant photoplethysmographic signal input subsystem

The photoplethysmographic signal analog input subsystem is made up from two components: a light flux transmitter controlled by the processor Figure 3.12 and a receiver Figure 3.13.

PSIS transmitter. The transmitter is made up from a swap voltage generator (*VoltGen*), sample-hold device (S/H), shift registry for optical Barker code storage, voltage level converter (LC), converter voltage – current (CVC), LED D1.

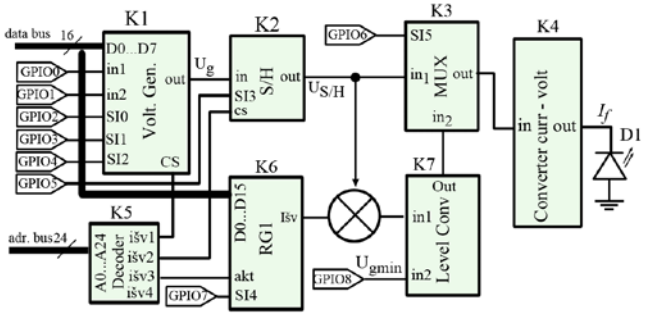

Figure 3.12 Structure of a transmitter of the photoplethysmographic signal input subsystem

The *sample-hold device* (K2) registers the value of VoltG output voltage. *Optical Barker code generator* is made from a shift registry (K6). Code values, one bit at a time, are transmitted to an analog multiplication device where the values of logical *"0"* and *"1"* are multiplied by $U_{S/H}$ voltage. In this way, the optical Barker code amplitude is modulated. The *voltage level converter* (K7) is an analog device designated to ensure that each swap voltage period would begin with a minimum voltage value U_{gmin} set during the automatic parameter setting procedure. The *converter voltage – current* (K4) converts the voltage produced by the transmitter subsystem and found in K3 output into a current f_{foto} of the light flux generating diode D1.

The optical signal received by the receiver of the photoplethysmographic signal input subsystem Figure 3.13 is enhanced and then sent to the analog correlation calculation device K10. This device calculates the correlation function of the signals found in inputs K10.in1 and K10.in2.

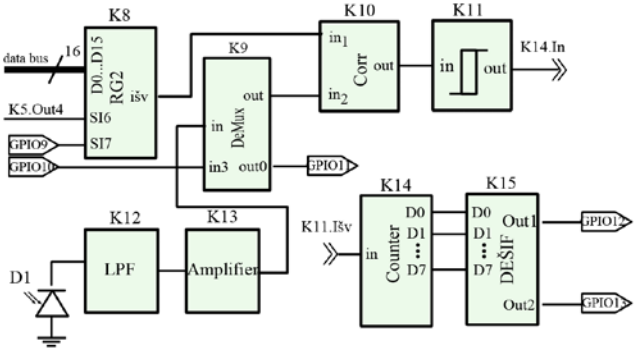

Figure 3.13 Structure of a receiver of the photoplethysmographic signal input subsystem

When the correlation spike exceeds the threshold voltage, the analog comparison device K11 creates an impulse signal. The counter K14 counts these signals.

Decoder K15 evaluates the number in the output of the counter, and if the number is larger than *"1"*, then a logical *"1"* is formed in the K15.out2 output, and in K15.out1 – a logical *"0"*. If the number is equal to *"1"*, then a logical *"0"* is formed in the output K15.out2, and in K15.out1 – a logical *"1"*.

3.4.1. Assessment of Energy Consumption of the Photoplethysmographic Signal Input Subsystem

Wearable systems used for long-term hemodynamic parameter monitoring have limited energy resources. Therefore, it is important to evaluate the energy consumption of the proposed system and to determine the duration of time the system can operate continuously without change of batteries.

A study of energy consumption of each functional block of the analog input subsystem of the proposed WHPMS is conducted in this chapter.

Energy consumed by the transmitter of the photoplethysmographic signal input subsystem (PSIS) is made up from a voltage-controlled swap voltage generator, selection-retention device (S/H), shift registry for optical Barker code storage, voltage level converter (LC), converter voltage – current, LED D1.

Current used by the swap voltage generator is $I_{gen} \leq 13\mu A$, current used by the control components (K2 – K7) of the transmitter is $I_{trans\_ctrl} \leq 95.02\mu A$, current used by the LED is $I_{LED} \leq 4.075\ \mu A$.

Total amount of energy used by the PSIS transmitter:

$$I_{trans} \leq I_{trans\_ctrl} + I_{LED} \leq 95.02 + 4.075 \leq 100\mu 0\ . \qquad (3.12)$$

Energy consumed by the receiver of the PSIS. Energy consumed by the photodiode is very low compared to other system components, therefore, it is not taken into consideration. Other subsystem components operate under a steady regime. Energy consumed by the sensor can be calculated in the following way:

$$I_{sens} = I_{amplif} + I_{LPF2} = 40\mu A + 20\mu A = 60\mu A. \qquad (3.13)$$

Total amount of energy used by the *PSIS* receiver:

$$I_r = I_{sens} + I_{K8} + I_{K9} + I_{K10} + I_{K11} + I_{K14} + I_{K15} =$$

$$= 60\mu A + 4\mu A + 0.9\mu A + 66\mu A + 60\mu A + 488\mu A + 20\mu A \leq 699\mu A. \qquad (3.14)$$

Energy consumed by the photoplethysmographic signal input subsystem created by the author and controlled by the processor:

$$I_{PSIS} \le I_t + I_r \le 100\mu A + 699\mu A \le 800\mu A\,. \qquad (3.15)$$

Conclusion. Analysis shows that the total amount of energy consumed by the photoplethysmographic signal input subsystem created by the author is 1.8mA/0.8mA = 2.5 times lower than the energy consumed by standard ADC integrated in a processor.

3.4.2 Assessment of the Effect the Developed Mathematical Models Have On the Energy Consumption of the Wearable Hemodynamic Parameter Monitoring System

Mathematical models created by the author enable the calculation of hemodynamic parameters by analyzing only the front edge of the PPG. Duration of the front edge takes up 1/5 of the entire cardiac cycle T_{HR} (Heart Rate period). If T_{HR} = 1s, then the amount of time for PPG front edge data input and analysis is T_{ed} = 0.2s (PPG front edge duration). For the rest of the cardiac cycle the system goes into "sleep" mode, which can be terminated only in the event of interface-to-user query.

In order to solve a filtering task with a RIR L = 64 filter, the clock frequency of the processor has to be F_{proc} = 12.3MHz. Given the technical characteristics of the selected processor MSP430F2x (current in active mode I_{proc} = 200μA/MHz), the electric current strength to run the filtering algorithm is I_{proc} = F_{proc} × 200 = 2.46mA. Energy usage of a LED operating in pulse regime (I_{LED} = 100mA, F_{LED} = 1KHz, duty cycle takes up 20%) is I_{LED} = 225μA. Total amount of energy used to calculate hemodynamic parameters per cardiac cycle E_{sist_1} is: E_{sist_1} = I_{proc} + I_{ADC} + I_{LED} = 2.4mA + 1.8mA + 0.225mA ≈ 4.5mAh.

When T_{HR} =1s, then the amount of time for PPG front edge data input and analysis is T_{ed} = 0.2s. For the rest of the cardiac cycle the system goes into "sleep" mode. In this case, the energy consumed by the system is E_{sist_2} = E_{sis_1}/5 = 0.9mAh. When processing only the front edge, energy consumption is reduced by E_{sist_1} / E_{sist_2} = (4.5/0.9) = 5 times.

3.5. Conclusions

1. The created mathematical models and results from modeling done in MatLab show that steepness values of the DPW front edge have a strong correlation with the DPW propagation speed and, therefore, can be used to assess arterial stiffness. When mathematical models developed by the author are used, the blood pressure value deviation does not exceed the limits set by the BHS (British Hypertension Society), and therefore can be used for blood pressure monitoring.
2. Mathematical models that link the front edge of a DPW (constituting 1/5 of the entire DPW) with hemodynamic parameters, allows decreasing

the duration of active operation time of the processor installed in the hemodynamic parameter monitoring system significantly and in doing so, reduces the amount of energy needed for signal filtering and analysis by up to 80%.

3. The suggested method of DPW foot approximation with lines is noise-resistant and is able to determine the starting point of the DPW front edge with accuracy of ±6ms when the signal-noise ratio is 18dB.
4. When the transmitter of the input subsystem generates a light flux modulated with an optical Barker code, the correlation of the received APW in the photo-receiver signal and the reference value is r= 0.98, even when the signal-noise ratio is 0dB. Light flux modulation with the optical Barker code (from N = 15 optical Barker code values only 5 are equal to "*1*") not only improves noise resistance but also decreases the amount of energy consumed by the sensor by ~50% as compared to conventional, impulse-based photoplethysmographic sensors.

4. EXPERIMENTAL STUDY OF CALCULATION METHODS FOR ARTERIAL BLOOD PRESSURE AND PULSE WAVE PROPAGATION SPEED

Experiments and equipment used for the verification of mathematical models created by the author to measure blood pressure and the PWV are described in this chapter.

4.1. Experimental Study of Methods for Arterial Blood Pressure and Deformation Pulse Wave Propagation Speed Calculation

A prototype WHPMS Figure 4.1 was used for experimental study of calculation methods for arterial blood pressure and DPW propagation speed when the steepness values of the front edge are used. The prototype has the following components: photoplethysmographic input subsystem, a STM32373 evaluation board with an integrated electrocardiograph and a 16-bit (F_d = 1KHz) analog-to-digital converter.

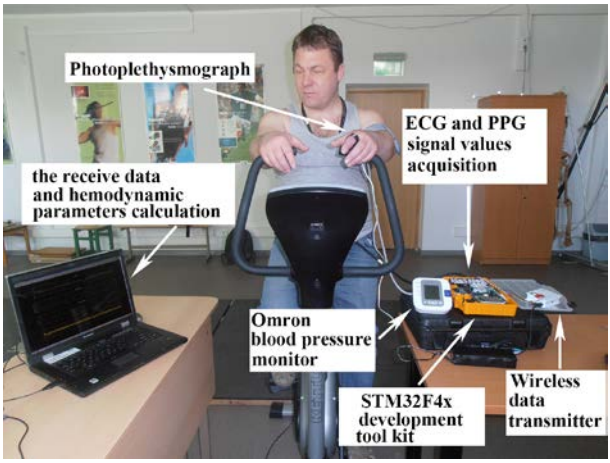

Figure 4.1 Equipment used during experimentation: a KETTLER veloergometer, semi-automatic blood pressure measuring device OMRON and the WHPMS prototype

A physical activity test was carried out to provoke changes in hemodynamic parameters (heart rate, pulse wave propagation speed, arterial blood pressure) by using a KETTLER veloergometer Figure 4.1.

Goal of the experiment was to verify the methods created by the author for systolic blood pressure and PWV measurement.

Experiment results of arterial blood pressure measurement by using the steepness values of the DPW front edge. Results in Table 4.1 show that the γ_{max_i} values, produced during modeling and experimentation, differ by a

constant: the alteration of modelled γ_{max_i} values reached about 1 degree, whereas the alteration of γ_{max_i} values gathered during experimentation was 1/1000 of a degree.

Table 4.1 DPW front edge steepness values gathered during modeling and experimentation at different blood pressure values

Blood pressure mmHg	DPB steepness γ_{max_i} (degree)	
	Modeling results	Measurement results
150 - 180	85.8 - 86.6	89.998±0.0003
135 - 155	84.8 - 85.1	89.996±0.0006
120 - 135	83.4 - 84.0	89.994±0.0008
110 - 120	82.0 - 82.8	89.992±0.0004

Correlation between the systolic blood pressure and the steepness values of the front edge of the PPG observed during experimentation is considerable – 0.955±0.025 ($p < 0.001$). Experimental results are consistent with modeling results and confirm the assumption that the change of trajectories of the front edges of both the pressure pulse wave and the deformation pulse wave coincides.

Modeling and experimentation results show that it is enough to measure the PPG and calculate the steepness values of the front edge in order to determine the dynamics of blood pressure.

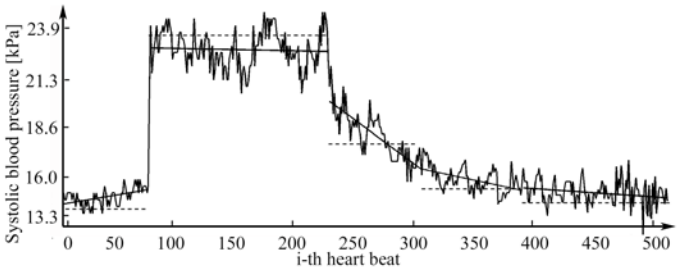

Figure 4.2 A diagram of systolic values measured with a standard device (dotted line) and with the proposed method (curved line). Calculated systolic blood pressure values are approximated with the adaptive mean square method $y_i(j)$ (bold broken line)

The proposed method can be used to calculate the systolic blood pressure values as well. Calculated blood pressure values p_j were approximated with the adaptive mean square method (bold broken line, Figure 4.2):

$$y(j) = a_i \times j + b_i \tag{4.1}$$

here – $y_i(j)$ is the approximated p_j values in the *i-th* segment ($\dim(y_i)$ = kPa).

Measured (p_i) and calculated (y_i) values are compared by calculating the mean of their differences with absolute value $\left|\overline{\Delta}\right| = E[|(y_i(j) - p_i)|]$, (where i=1…4, j=1…N) and standard deviation is $s.d_{\Delta}$. Results show that in all cases the standard deviation of differences (scatter) is lower than 8mmHg. Therefore, the proposed method meets the AAMI and BHS standards and is suited for use in wearable, personal blood pressure monitoring devices.

Results of experimental determination of the pulse wave propagation time by using the steepness of the DPW front edge. Typical *PTT(n)* and *φ(n)* curves Figure 4.3 are observed during experimentation. A significant correlation of -93.4± 5.6 is observed between *PTT(n)* and *φ(n)*.

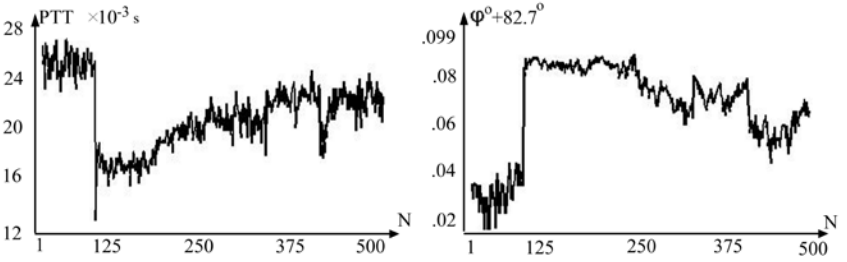

Figure 4.3 Typical curves produced during experimentation: a) longitudinal *DPW* propagation time curves and b) curves of lateral *DPW* propagation speed $v_r(n)$ expressed in degrees.

In order to compare PTT and $v_r(n)$, veloergometer test results were analyzed. *PTT(n)* and *φ(n)* sequences were standardized. After standardizing, the variation interval of *PTT*(n) values was $0 \le PTT(n) \le 1$, and the variation interval of *φ(n)* values was $0 \le \varphi(n) \le 1$. Comparison results, as seen in Table 4.2, show that the difference between standard values is small, therefore, one method can be replaced by another one.

Table 4.2 Comparison of standard *PTT(n)* and *φ(n)* values

method	average	standard deviation	p
PBSL(n)	0.6 ± 0.15	0.1±0.57	$< 10^{-5}$
φ(n)	0.7±0.13	0.06±0.37	$< 10^{-5}$

Experiment results show that the pulse wave propagation time can be replaced by steepness values of the pulse wave front edge that are measured with a photoplethysmograph.

CONCLUSIONS

1. In contrast to non-invasive hemodynamic parameter monitoring systems that register PPW, systems that use a photoplethysmographic DPW recording method have no restrictions that would hinder a continuous 24/7 real-time monitoring of hemodynamic parameters. However, in these systems, more than 80% of all energy resources are used for analog-to-digital conversion and adaptive filtering of the photoplethysmographic signal. This reduces the time of continuous monitoring significantly and, therefore, requires solutions that would extend the operation time.
2. Mathematical models that link the front edge of an APW (constituting 1/5 of the entire APW) and hemodynamic parameters, allow decreasing the duration of active operation regime of the processor installed in a hemodynamic parameter monitoring system significantly and in doing so, reduces the amount of energy needed for signal filtering and analysis by up to 80%.
3. A precise identification of the starting point of an APW is necessary in order to find APW front edge parameter values. A method developed by the author for pulse wave foot approximation with lines allows determination of the starting point of the APW with a ±6ms accuracy when signal-noise ratio is 18dB.
4. When an input subsystem transmitter generates a light flux modulated with an optical Barker code, the correlation of the received APW in the photo-receiver signal and the reference value is r= 0.98, even when signal-noise ratio is 0dB. Light flux modulation with an optical Barker code (from N = 15 optical Barker code values only 5 are equal to “1”) not only improves noise resistance but also reduces the amount of energy consumed by the sensor by ~50% as compared to conventional, impulse-based photoplethysmographic sensors.
5. In order to increase the duration of continuous hemodynamic parameter monitoring in wearable systems, solutions are needed that would allow avoiding continuous real-time filtering and the standard use of ADCs. WHPMS structure with a noise-resistant photoplethysmographic signal input subsystem and a functional WHPMS algorithm is created and explained in this paper. Here, instead of ADC, amplitude-time converter is used, while the noise-resistant input subsystem allows dropping the continuous real-time filtering function. Once ADC and continuous real-time filtering is no longer used, the system consumes only 20% of energy for solving the same task as compared to conventional methods.

PUBLICATIONS

Indexed in the Web of Science with Impact Factor

1. Girčys, R., Liutkevičius, A., Vrubliauskas, A., & Kazanavičius, E. (2015) Blood pressure estimation according to photoplethysmographic signal steepness. Information technology and control, 44(4), p. 443-450.
2. Girčys, R., Kazanavičius, E., Vrubliauskas, A., & Liutkevičius, A. (2014). Movement artefact resistant photoplethysmographic probe. Electronics and Electrical Engineering, 20(3), 73-76.

Publications in other international databases

1. Girčys, R., Kazanavičius, E., Obcarskas, L. (2013) Arterial pulse transit time evaluation by peripheral pulse wave measurement. Journal of measurements in engineering, 1(1), p. 52-58.
2. Kazanavičius, E., Girčys, R., Vrubliauskas, A., & Lugin, S. (2005) Mathematical methods for determining the foot point of the arterial pulse wave and evaluation of proposed methods. Information technology and control, 34(1), p. 29-36.

Articles in periodicals, collections of articles, etc.

1. Girčys, R., Kazanavičius, E., Lugin, S., & Vrubliauskas, A. (2004) Mathematical model of the aortic root pressure waveform as an input function of the arterial system. Mechanika, 2(46), p. 42-45.

INFORMATION ABOUT THE AUTHOR

2013 – 2015	Researcher in project “Research on Smart Home Environment and Development of Intelligent Technologies (BIATech)” (Project No. VP1-3.1-ŠMM-10-V-02-0200, Kaunas University of Technology). During project implementation, employed as a Junior Researcher at the Centre of Real Time Computer Systems, Faculty of Informatics, Kaunas University of Technology.
2012 – 2013	Project researcher in a project sponsored by Agency for Science, Innovation and Technology (MITA), project Nr. VP2-1.3-ŪM-05-K-01-147, 2013 “Research and development of human-machine interfaces using computational intelligence techniques”.
2008 – present	Full time lecturer at the Department of Computer Sciences, Faculty of Informatics, Kaunas University of Technology.
2005 – 2008	Assistant at the Department of Computer Sciences, Faculty of Informatics, Kaunas University of Technology.
2000 – 2005	Completed doctoral studies in Informatics Engineering (07T). Kaunas University of Technology.
1998 – 2000	Master’s degree with honors in Informatics Engineering (07T). Kaunas University of Technology.
1994 – 2000	Junior Researcher at Palanga Psychophysiology and Rehabilitation Institute, Kaunas University of Medicine (now – LSMU, Lithuanian University of Health Sciences).
1993 – 1994	Acquired a Certified Engineer degree. Kaunas University of Technology.
1989 – 1993	Bachelor’s degree in Engineering. Kaunas University of Technology.

REZIUMĖ

Tyrimo objektas

Šiame darbe nagrinėjamos neinvazinės kraujotakos parametrų stebėjimo sistemos ir apdorojimo metodai.

Temos aktualumas

Pagrindinė problema su kuria susiduriama kuriant nenutrūkstančiam 24v/7d kraujotakos parametrų stebėjimui skirtas, kasdienės veiklos metu dėvimas sistemas – *riboti skaičiavimo ir energijos resursai*. Tokios sistemos (laikrodis, apyrankė akiniai ir kt.) atlieka ne tik funkcinę, bet ir estetinę paskirtį, todėl sistemos dydis riboja energijos ir skaičiavimo resursų išteklius kurie gali būti naudojami sistemos funkcijai realizuoti.

Šiandien rinka pristato įterptinėms sistemoms skirtus, našius signalų apdorojimo procesorius ir didelę skiriamąją gebą bei diskretizavimo dažnį turinčius analoginius – skaitmeninius keitiklius. Analoginio signalo keitimui į skaitmeninį ir skaitmeninio signalo apdorojimui sunaudojama didžioji visos sistemos skaičiavimo ir energijos resursų dalis. Tai ženkliai mažina nenutrūkstamo kraujotakos parametrų stebėjimo laiką, todėl reikalingi nauji sprendimai, suteikiantys galimybę realizuoti kasdienės veiklos metu dėvimas, nenutrūkstančio 24v/7d arterinės sistemos būklės stebėjimo sistemas. Tokie sprendimai apima: 1) APB parametrų, kurių reikšmėms skaičiuoti reikia mažiau skaičiavimo resursų nei dabar naudojamų parametrų reikšmėms rasti, paiešką 2) APB ir kraujotakos parametrus siejančių matematinių – fizikinių modelių sukūrimą, 3) atsparių triukšmui analoginio signalo įvesties posistemių nenaudojančių ASK sukūrimą, 4) triukšmui atsparių metodų APB parametrų reikšmėms rasti sukūrimą.

Minėtų uždavinių sprendimai glaudžiai susiję su dėvimų kraujotakos stebėjimo sistemų sukūrimu, tačiau jie gali būti panaudoti ne tik medicinoje, bet ir kitose srityse.

Tikslas ir uždaviniai

Darbo tikslas arterinės pulsinės bangos analizės metodų, skirtų kraujotakos parametrams skaičiuoti, ir realaus laiko nenutrūkstamo 24/7 kraujotakos parametrų stebėjimo sistemos su triukšmui atsparia signalo įvesties posisteme sudarymas ir tyrimas.

Sprendžiami uždaviniai:

1. Atlikti neinvazinių kraujotakos parametrų stebėjimo ir apdorojimo sistemų apžvagą ir analizę.
2. Sukurti matematinius modelius siejančius kraujotakos ir APB priekinio fronto parametrus.
3. Sukurti triukšmui atsparius būdus APB priekinio fronto parametrų reikšmėms rasti.
4. Sukurti triukšmui atsparios, energiją taupiai eikvojančios signalo įvesties posistemės struktūrą ir funkcionavimo algoritmą.
5. Sukurti dėvimos, realaus laiko kraujotakos parametrų stebėjimo ir apdorojimo sistemos struktūrinį modelį.

Tyrimų metodika

Kraujotakos parametrų skaičiavimo metodų eksperimentiniam verifikavimui atliekamas veloergonometrinis testas (fizinio krūvio mėginys) kurio metu registruojama fotopletizmograma, elektrokardiograma ir kraujospūdis.

Mokslinis naujumas

1. Sukurti matematiniai modeliai siejantys APB priekinio fronto statumą su jos sklidimo greičiu ir arteriniu kraujospūdžiu.
2. Pasiūlytas naujas APB pradžios taško nustatymo būdas kurį taikant gaunamos tikslesnės rezultatų reikšmės ir mažesnis jų išsibarstymas nei taikant žinomus metodus.
3. Pasiūlyta nauja, triukšmui atspari fotopletizmografinio signalo įvesties posistemės struktūra.

Ginamieji teiginiai

1. Deformacijos pulsinės bangos priekinio fronto statumas koreliuoja su jos sklidimo greičiu ir kraujospūdžiu.
2. Analizuojant tik priekinį APB frontą, kraujotakos parametrų reikšmėms rasti, sumažėja energijos sąnaudos.
3. Fotopletizmografinio jutiklio naudojamas optiniu Barkerio kodu moduliuotas šviesos srautas leidžia ženkliai sumažinti triukšmo lygį jutiklio išvesties signale ir atsisakyti nenutrūkstamo, skaitmeninio signalo filtravimo, ko pasėkoje sumažinamas dėvimos sistemos energijos suvartojimas.

4. Analoginį – skaitmeninį keitiklį pakeitus keitikliu „šviesos srautas – laikas“ sumažinamas dėvimos sistemos energijos suvartojimas.
5. Tiesėmis aproksimuojant arterinės pulsinės bangos papėdę ženkliai sumažinama triukšmo įtaka APB pradžios nustatymo rezultatams.

Praktinė reikšmė

Fotopletizmografiniam periferinės kraujotakos registravimo metodui galima naudoti šiuolaikinius puslaidininkinius šviesos šaltinius ir jutiklius, kurie yra saugūs, maži ir ekonomiški. Toks metodas geriausiai atitinka reikalavimus keliamus prietaisams, skirtiems naudoti ambulatorinėmis ir namų sąlygomis.

Šiame darbe sukurtos arterinės pulsinės bangos priekinio fronto analizės metodai bei moduliuotos šviesos srauto fotopletizmografinis jutiklis suteikia platesnes galimybes dėvimose sistemose racionaliau naudoti tokius kritinius resursus kaip energijos suvartojimas ir skaičiavimo resursai.

Darbo aprobavimas

Darbo rezultatai pritaikyti būsto išmaniosios aplinkos kūrimo programinėje įrangoje, sukurtoje pagal projektą „Būsto išmaniosios aplinkos tyrimai ir intelektualių technologijų kūrimas – BIATech“ VP1–3.1–ŠMM–10–V–02–020.

Darbo rezultatai pritaikyti įgyvendinant projektą pagal VP2-1.3-ŪM-05-K priemonę „INOČEKIAI LT“ „Taikomųjų sąsajų žmogus – mašina kūrimas ir tyrimai taikant skaitinio intelekto metodus“.

Disertacijos darbo tema paskelbtos publikacijos:

Web of Science duomenų bazės leidiniuose su citavimo indeksu

1. Girčys, R., Liutkevičius, A., Vrubliauskas, A., & Kazanavičius, E. (2015) Blood pressure estimation according to photoplethysmographic signal steepness. Information technology and control, 44(4), p. 443-450.
2. Girčys, R., Kazanavičius, E., Vrubliauskas, A., & Liutkevičius, A. (2014). Movement artefact resistant photoplethysmographic probe. Electronics and Electrical Engineering, 20(3), 73-76.

Kitų tarptautinių duomenų bazių leidiniuose

1. Girčys, R., Kazanavičius, E., Obcarskas, L. (2013) Arterial pulse transit time evaluation by peripheral pulse wave measurement. Journal of measurements in engineering, 1(1), p. 52-58.
2. Kazanavičius, E., Girčys, R., Vrubliauskas, A., & Lugin, S. (2005) Mathematical methods for determining the foot point of the arterial pulse wave and evaluation of proposed methods. Information technology and control, 34(1), p. 29-36.

Periodiniuose leidiniuose ir vienkartiniuose straipsnių rinkiniuose ir kt. paskelbti straipsniai

1. Girčys, R., Kazanavičius, E., Lugin, S., & Vrubliauskas, A. (2004) Mathematical model of the aortic root pressure waveform as an input function of the arterial system. Mechanika, 2(46), p. 42-45.

Darbo struktūra

Disertacinis darbas susideda iš įvado, keturių skyrių, disertacijos išvadų, literatūros sąrašo ir priedų. Bendra disertacijos apimtis – 115 puslapių.

Darbo turinys. Įvade pagrindžiama tiriamoji problema, apibrėžiamas darbo aktualumas, tikslas, uždaviniai, darbo naujumas ir jo reikšmė. Pateikiami disertacijos ginamieji teiginiai.

Neinvazinio spaudimo ir deformacijos pulsinių bangų registravimo bei kraujotakos parametrų skaičiavimo metodų apžvalga ir analizė pristatoma ***antrame skyriuje***.

Dėvimose 24v/7d realaus laiko sistemose, kraujotakos parametrų skaičiavimas atliekamas apdorojant visas į kardiociklą patenkančias reikšmes. Tai neracionalu skaičiavimo resursų (o tuo pačiu ir energijos suvartojimo) požiūriu. Todėl reikalingi matematiniai – fizikiniai modeliai, kurie sieja norimus stebėti kraujotakos parametrus su mažesniosios arterinės pulsinės bangos dalies – priekinio fronto parametrais.

Trečio skyriaus pirmame poskyryje pristatomi autoriaus sudaryti matematiniai – fizikiniai modeliai, siejantys arterinės pulsinės bangos priekinio fronto ir kraujotakos parametrus.

Dėvimose 24v/7d realaus laiko sistemose įdiegus autoriaus siūlomus matematinius modelius gaunamas žymus energijos resursų taupymas, nes priekinio fronto trukmė sudaro ne daugiau kaip 1/5 visos pulsinės bangos, o likusias 4/5 kardiociklo dalis sistema gali būti „miego“ būsenoje. Sumažėja apdorojamų duomenų kiekis, ko pasėkoje gali būti naudojamas mažesnės vidinės atminties procesorius, o taip pat parinktas mažesnis procesoriaus taktinis dažnis. Kadangi APB priekinis frontas yra greičiausiai kintanti analizuojamo signalo dalis, tai ji mažiausiai įtakojama triukšmo, todėl tampa paprastesnis signalo paruošimo analizei uždavinys.

Autoriaus sukurti matematiniai modeliai skirti APB priekinio fronto analizei todėl svarbus APB pradžios nustatymo uždavinys.

Trečio skyriaus antrame poskyryje pristatomi fotopletizmografinio signalo (FPGS) pradžios taško nustatymo metodai realizuojami DKPSS skaitmeninės informacijos apdorojimo posistemėje. Atlikta triukšmo įtakos rezultatų tikslumui ir glaudumui analizė.

Trečio skyriaus trečiame poskyryje aprašyta fotopletizmografinio signalo įvesties posistemė, kurios dėka ženkliai sumažinamas triukšmo lygis FPGS

jutiklio išvestyje. Pristatomas algoritmas „šviesos srautas – laikas“ leidžiantis atlikti signalo skaitmenizavimą atsisakant standartinio ASK.

Trečio skyriaus ketvirtame poskyryje aprašoma DKPSS struktūra su triukšmui atsparia, FPGS analoginės įvesties posisteme. Pateikiama įvesties posistemės energijos suvartojimo analizė ir sudarytų matematinių modelių įtaka DKPSS vartojamai energijai tyrimas.

Ketvirto skyriaus pirmame poskyryje aprašomas DKPSS prototipas su jame realizuotais, autoriaus sukurtais kraujospūdžio ir PBG skaičiavimo matematiniais modeliais.

Ketvirto skyriaus antrame poskyryje aprašomas eksperimentas skirtas autoriaus sukurtiems kraujospūdžio ir PBG skaičiavimo matematiniams modeliams verifikuoti. Pateikti eksperimento rezultatai bei išvados apie rezultatų gautų pasiūlytais ir žinomais metodais atitikimą.

UDK 004.031.43+612.13](043.3)

SL344. 2016-09-12, 2,5 leidyb. apsk. l. Tiražas 50 egz. Užsakymas 325.
Išleido Kauno technologijos universitetas, K. Donelaičio g. 73, 44249 Kaunas
Spausdino leidyklos „Technologija“ spaustuvė, Studentų g. 54, 51424 Kaunas